Photoluminescence sidebands of carbon nanotubes below the bright singlet excitonic levels

Yoichi Murakami,[1,*,†] Benjamin Lu,[2] Said Kazaoui,[3] Nobutsugu Minami,[4] Tatsuya Okubo,[1] and Shigeo Maruyama[5,*,‡]

[1]*Department of Chemical System Engineering, The University of Tokyo, Bunkyo-ku, Tokyo 113-8656, Japan*
[2]*Department of Bioengineering, Rice University, Houston, Texas 77005, USA*
[3]*Nanotube Research Center, National Institute of Advanced Industrial Science and Technology, Tsukuba, Ibaraki 305-8565, Japan*
[4]*Nanotechnology Research Institute, National Institute of Advanced Industrial Science and Technology, Tsukuba, Ibaraki 305-8565, Japan*
[5]*Department of Mechanical Engineering, The University of Tokyo, Bunkyo-ku, Tokyo 113-8656, Japan*

We performed detailed photoluminescence (PL) spectroscopy studies of three different types of single-walled carbon nanotubes (SWNTs) by using samples that contain essentially only one chiral type of SWNT, (6,5), (7,5), or (10,5). The observed PL spectra unambiguously show the existence of an emission sideband at ~ 140 meV below the lowest singlet excitonic (E_{11}) level, whose identity and origin are now under debate. We find that the energy separation between the E_{11} level and the sideband is independent of the SWNT diameter within our experimental certainty. Based on this, we ascribe the origin of the observed sideband to coupling between K-point phonons and dipole-forbidden dark excitons, as recently suggested based on the measurement of (6,5) SWNTs.

I. INTRODUCTION

The optical and electronic properties of one-dimensional (1D) materials have been an important subject in the field of condensed matter physics.[1,2] The enhanced Coulomb interactions in 1D often lead to the formation of strongly bound electron-hole (*e-h*) pairs called excitons.[3] It is known that the optical properties of 1D semiconductors are distinctly different from higher-dimensional materials, being inherently dominated by excitons.[4,5] The sharp spatial localization of strongly bound excitons often makes the exciton-phonon (ex-ph) interaction important.[6]

Single-walled carbon nanotubes (SWNTs) (Ref. 7) are 1D materials that possess various unique properties.[8] The strong confinement in the radial direction (~ 1 nm) and the weak dielectric screening inside SWNTs give rise to very large exciton binding energies of ~ 0.5 eV,[9–13] which is much larger than those of InGaAs quantum wires[5,14] and larger than or comparable to those of π-conjugated polymers.[15,16] So far, various groups have studied the ex-ph interactions in SWNTs both in terms of theory[17,18] and experiment[19–22] and have revealed the existence of a phonon sideband approximately 200 meV above the energy level of the singlet bright exciton (which has an *s* envelope and termed a "1*u*" state based on symmetry[12,13] but we simply call it "E_{ii}" hereafter for the *i*th single-particle subband).[17–22]

Techniques for preparing SWNT samples for optical studies have been rapidly improving recently. A technique that utilizes fluorene polymers to disperse SWNTs in organic solvents reported by Nish *et al.*[23] is considered to be particularly important because of the strong selectivity to specific chiral types of SWNTs. The density gradient separation method reported by Arnold *et al.*[24,25] is another important technique that separates SWNTs according to their diameters as well as to their metallic/semiconducting property.

In this paper, we performed detailed photoluminescence (PL) spectroscopy studies of three different types of SWNTs [(6,5), (7,5), and (10,5)] using samples containing virtually only one type of SWNT, and unambiguously show the existence of emission sidebands at approximately 140 meV below the E_{11} level for all of these SWNT types. Currently, the physical origin of this sideband is under debate: this sideband was initially discovered by Kiowski *et al.*,[26] who explained its origin as "deep dark excitonic states." They ruled out the possibility of a phonon-dissipating emission mechanism based on their experimental observation that the energy separation between the E_{11} level and the sideband (δ) is remarkably dependent on SWNT diameter (d_{SWNT}). On the other hand, Torrens *et al.*[27] recently proposed that this sideband originates from dipole-forbidden "dark" excitons coupled with K-point phonons (i.e., the mechanism that was ruled out in Ref. 26) based on their experimental measurement limited only to (6,5) SWNTs. Apparently, the dependence of δ on d_{SWNT} is a key issue to resolve this conflict, which is essential for correctly understanding the properties of the weak photoemission found below the E_{11} states.

II. EXPERIMENTAL RESULTS AND ANALYSIS

We prepared three types of samples, denoted as "DG," "PFO," and "PFO-BT." In essence, the first sample was prepared based on the density-gradient separation method,[25,28] and the latter two samples utilized fluorene polymers to individually disperse SWNTs in toluene.[23] Details of the sample preparation procedures are described separately.[29] Although our samples may contain some amount of metallic SWNTs, since they do not emit PL,[30] the possible existence of metallic SWNTs does not affect our results and discussion presented here.

Figure 1 shows colored contour maps of the PL excitation intensities measured from the [(a) and (d)] DG, [(b) and (e)] PFO, and [(c) and (f)] PFO-BT samples. Panels (d)–(f) are the same as panels (a)–(c), but the intensities are presented in logarithmic scale. This figure shows that the samples contained virtually only one chiral type of SWNTs while the amounts of other types of SWNTs were highly suppressed.
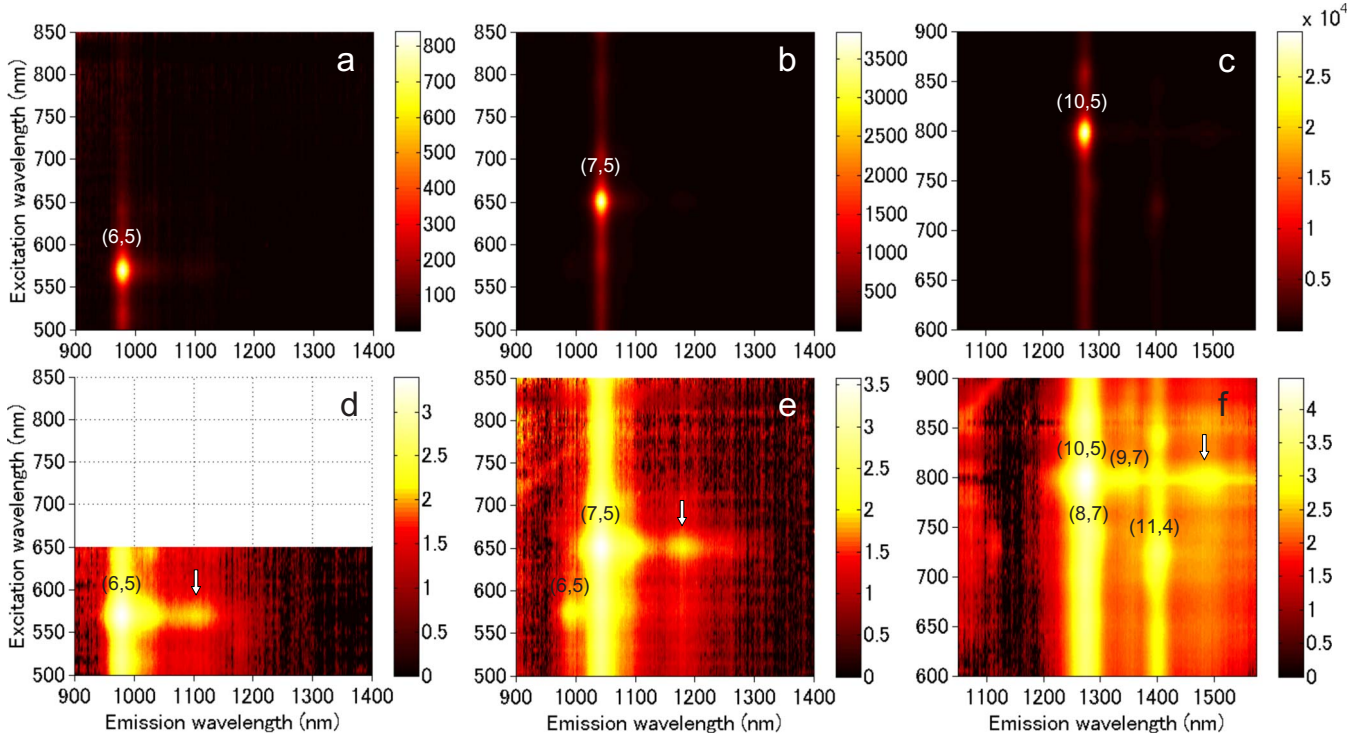
FIG. 1. (Color online) Contour maps of PL excitation intensities measured from the [(a) and (d)] DG, [(b) and (e)] PFO, and [(c) and (f)] PFO-BT samples. Intensity scale bars are attached to the right of each panel, where the unit is photon count. Panels (d)–(f) are the same as panels (a)–(c), but the intensities are shown in log scale. Arrows indicate the locations of the sidebands.

Panels (d)–(f) clearly show the existence of sidebands (indicated by the arrows) associated with the PL features of (6,5), (7,5), and (10,5) SWNTs, respectively.

Figures 2(a)–2(c) show PL spectra measured from the DG, PFO, and PFO-BT samples obtained by resonantly exciting E_{22} levels of the dominant SWNT species with excitation wavelengths 570, 655, and 800 nm, respectively. The abscissa denotes energy relative to the PL emission maxima from respective E_{11} levels. We performed spectral-decomposition analysis in order to obtain the positions and widths of the observed peaks. Specifically, we fit these spectra with an E_{11} PL peak, a shoulder at ~45 meV below the E_{11} level (see Fig. S3 in Ref. 29) and the PL sideband shown in Fig. 1. As for Fig. 2(c), additional peaks for (9,7) and (11,4) tubes were taken into account. We assumed a 50% Lorentzian+50% Gaussian line shape for all the peaks, and optimized both the positions and widths of the peaks to best reproduce the original spectra. In these figures, the blue dash curves show the summation of all the components which overlap the experimental spectra shown by the black solid curves. Uncertainties or the possible ranges of the peak-maximum position of the sidebands obtained from the decomposition analysis are indicated by horizontal bars shown in Figs. 2(a)–2(c), whose magnitudes are approximately 10 meV.

Figure 3(a) shows the peak widths full width at half maximum (FWHM) of the observed E_{11} PL emission features (solid circles) and sideband features (solid squares), which were obtained from the above fitting analysis, plotted as a function of d_{SWNT}. The decrease of the widths of the E_{11} PL emission features with the increase of d_{SWNT} agrees with the

behavior reported by Inoue *et al.*[31] Although the samples measured in this study were ensembles of SWNTs, the clear dependence of the E_{11} emission widths on d_{SWNT} indicates that these peaks were not completely smeared out by the ensemble effect. In fact, the widths (15–30 meV) are approximately twice of those measured from a single isolated SWNT at room temperature.[31] It is noted that the widths of the sideband features show a similar inverse dependence on d_{SWNT} and are always larger than those of the E_{11} features, which indicates that these features are not artifacts due to E_{11} PL emissions from other SWNTs with larger diameters.

The filled squares plotted in Fig. 3(b) represent the dependence of δ on d_{SWNT}, which shows that the observed δ is independent of d_{SWNT} (~140 meV, in the range of $0.75 \leq d_{SWNT} \leq 1.05$ nm) within the uncertainties indicated in Figs. 2(a)–2(c) [shown by error bars in Fig. 3(b)]. For comparison, the values of δ reported for the similar sidebands in Ref. 26 are plotted as open triangles in the same figure, with the experimental uncertainty of ±5 meV represented by the error bars. As described by the authors, their δ shows a remarkable dependence on d_{SWNT}, which is qualitatively different from our experimental observation, i.e., there is a clear difference between these two data sets that exceeds the uncertainties in both experiments. Kiowski *et al.*[26] explained that the observed PL sidebands were weak PL emission from deep dark excitonic states below the E_{11} levels, even lower than the energy level of the singlet dark exciton with zero angular momentum and an s-envelope [termed the "1g" exciton[12,13] and has energy ~5 meV lower than the E_{11} (or "1u") level[32–34]]. It is noted that these authors have ruled out the possibility of phonon-involved processes regarding
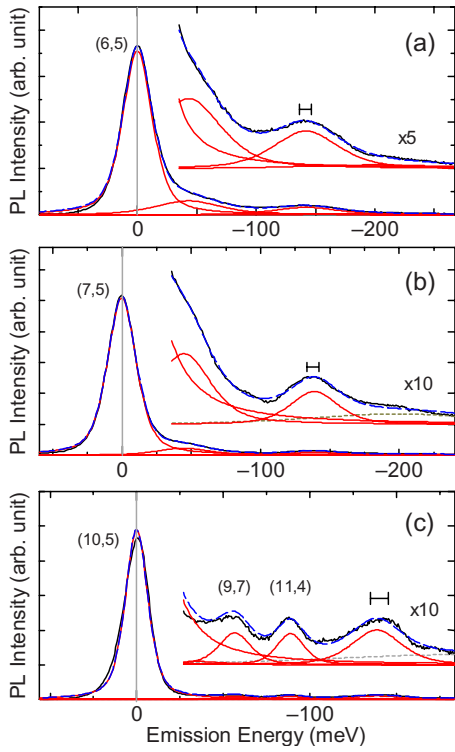
FIG. 2. (Color online) PL spectra measured from the (a) DG, (b) PFO, and (c) PFO-BT samples, obtained by resonantly exciting the E_{22} levels of the dominant SWNTs with excitation wavelengths of 570, 655, and 800 nm, respectively. The abscissa represents the energy relative to the E_{11} levels of (6,5), (7,5), and (10,5) SWNTs. The original spectra, shown by black solid curves, were decomposed into multiple peaks, and the summation is shown by blue dashed curves. The gray short-dash curves in (b) and (c) are spectral baselines assumed in the analysis. The uncertainties in the peak-maximum positions of the PL sidebands are indicated by the horizontal bars.

the origin of these sidebands based on the apparent dependence of δ on d_{SWNT}.[26] In contrast, the independence of δ on d_{SWNT} observed in this study suggests an involvement of phonons in the origin of these sidebands, particularly the involvement of higher-frequency (>1000 cm^{-1}) phonons that arise from the phonon dispersion relations of graphite,[35] and hence is essentially independent of d_{SWNT}. So far, the phonon sideband at ~ 200 meV above the E_{ii} levels has been well recognized and studied.[17–22] This phonon sideband was first predicted by Perebeinos *et al.*[17] as a result of strong coupling between dipole-forbidden excitons above the E_{11} level and K-point phonons (~ 170 meV). This phonon is known to possess an in-plane transverse optical (TO) mode and is responsible for the D-band Raman feature in graphite and carbon nanotubes through a one-phonon emission double-resonance Raman process.[35–37]

III. DISCUSSIONS

Figure 4 shows a schematic diagram that describes the four lowest-energy states of singlet excitons in SWNTs.[32] The abscissa denotes the momentum q of the excitons. The
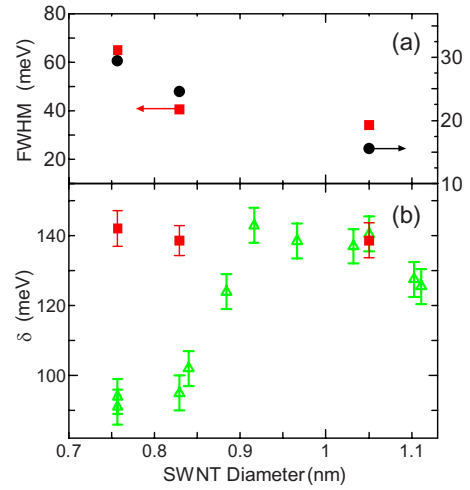

FIG. 3. (Color online) (a) Dependence of the peak widths FWHM of the E_{11} PL emissions (solid circles) and the observed sidebands (solid squares) on d_{SWNT}. The widths were obtained from the fitting analysis shown in Fig. 2. (b) Solid squares: the relationship between δ and d_{SWNT} measured in this paper. Magnitudes of the error bars are the same as widths of the horizontal bars shown in Figs. 2(a)–2(c). Open triangles: the relationship between δ and d_{SWNT} for similar PL sidebands reported in Ref. 26, where the error bars denote ± 5 meV experimental accuracy reported in the literature.

solid (dashed) curve represents the dipole-allowed (dipole-forbidden) excitonic state with zero angular momentum E_{11} (E_{1g}). The dot-dashed curve denotes the dipole-forbidden exciton band with finite angular momentum whose energy has been predicted to be approximately 20–30 meV higher than the E_{11} level for $q=0$.[32] We denote this energy separation by Δ as shown in Fig. 4. Only the $q \approx 0$ excitons in the E_{11} level can directly interact with photons. For simplicity, we have shown here the diagram for zigzag SWNTs,[32,38] but the gen-
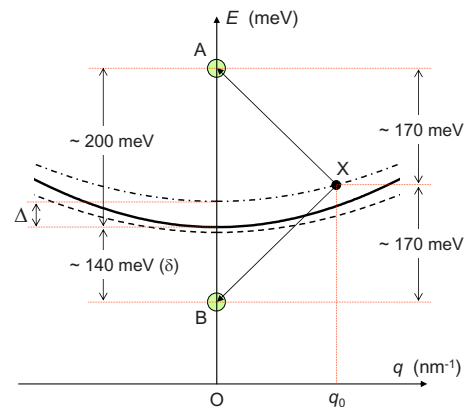

FIG. 4. (Color online) Schematic diagram showing the four lowest-energy singlet exciton states in SWNTs. The abscissa denotes the exciton momentum. The solid and dashed curves denote bright (E_{11}) and dark (E_{1g}) exciton bands with zero angular momentum, respectively. The dot-dashed curve denotes the dark exciton band with nonzero angular momentum. The arrow connecting the points X and B shows the process suggested for the PL sidebands observed in this study.

erality in the following discussion is not affected by this simplification. Based on this schematic, the phonon sideband predicted by Perebeinos *et al.*,[17] corresponds to the point *A*, emerging as a result of the scattering of the dark exciton at $q=q_0$ (point *X*) by *K*-point TO phonons with $q=-q_0$.

We explain the origin of the observed sideband at ~ 140 meV below E_{11} as follows based on the same model recently proposed by Torrens *et al.*[27] The strong coupling between dark excitons with finite angular momentum and *K*-point phonons (~ 170 meV $\equiv E_{ph}$) predicted by Perebeinos *et al.*[17] also causes the scattering of dark excitons at $q=q_0$ (at *X* in Fig. 4) into the bright excitonic state at $q=0$ (*B* in Fig. 4), reducing their energy by E_{ph} through emission of a *K*-point TO phonon of wave vector q_0, satisfying both the energy and momentum conservation requirements simultaneously. In this process, the phonon sideband is expected to appear at approximately 140 meV ($\cong 170-30$ meV) below the E_{11} level, which agrees well with our experimental results. We note that the sidebands disappeared at 6 K according to the results shown by Kiowski *et al.*,[26] and this seems to support the above phonon-mediated interpretation.

Here, we briefly describe the values of Δ for (6,5) and (7,5) tubes based on the values obtained for δ. To do this we need to know the energy differences between E_{11} levels and their PLE sidebands denoted by δ_{PLE}. We obtained δ_{PLE} for (6,5) and (7,5) from Fig. 2(a) in Ref. 30, which are approximately 212 and 209 meV, respectively. Using the relationship $\Delta=(\delta_{PLE}-\delta)/2$,[27] we obtained $\Delta=35\pm 5$ meV for both (6,5) and (7,5) SWNTs.

Finally, we estimate the possible effect of environmental difference in the three types of samples used in this study. As shown in Fig. S1 of Ref. 29, the E_{11} emission energies of (6,5) tubes in the PFO and DG samples differ by ~ 9 meV. (Our unpublished data show that the E_{11} energy difference of the same chirality tubes between "PFO" and "PFO-BT" samples is much smaller.) The exciton binding energy, the energy difference between the band gap and the E_{11} level, of (6,5) tubes is known to be ~ 400 meV.[13] This means that the overall Coulomb interaction that determines the magnitude of the *e-h* interaction is changed by $\sim 2\%$ due to the environment. By a first approximation, the magnitude of Δ is considered to be modified by a similar proportion. 2% of Δ (~ 35 meV) is 0.7 meV, which is the estimated difference in the value of Δ due to the environment. This is negligible compared to the magnitude of the error bars (~ 10 meV) shown in Fig. 3(b).

IV. SUMMARY

We have performed detailed PL studies of (6,5), (7,5), and (10,5) SWNTs by using samples that contain essentially only one chiral type of SWNT. Their PL spectra unambiguously show sideband features at ~ 140 meV below the E_{11} levels for all of these SWNT types. The experimental results showed that δ was almost independent of d_{SWNT} within the resolution of our data (± 5 meV). This result suggests that the observed sidebands emerge as a result of strong coupling between dark excitons with finite angular momentum and *K*-point TO phonons, in agreement with the recent suggestion by Torrens *et al.*[27] based on measurements of (6,5) SWNTs.

*Corresponding authors.

†Present address: Global Edge Institute, Tokyo Institute of Technology, 2-12-1 Ookayama, Meguro-ku, Tokyo 152-8550, Japan. murakami.y.af@m.titech.ac.jp

‡maruyama@photon.t.u-tokyo.ac.jp

[1] *Optical Properties of Low-Dimensional Materials*, edited by T. Ogawa and Y. Kanemitsu (World Scientific, Singapore, 1995).

[2] T. Giamarchi, *Quantum Physics in One Dimension* (Oxford University Press, New York, 2004).

[3] R. S. Knox, *Theory of Excitons* (Academic, New York, 1963).

[4] T. Ogawa and T. Takagahara, Phys. Rev. B **43**, 14325 (1991); **44**, 8138 (1991).

[5] F. Rossi and E. Molinari, Phys. Rev. Lett. **76**, 3642 (1996).

[6] Y. Toyozawa, *Optical Properties of Solids* (Cambridge University Press, Cambridge, 2003).

[7] S. Iijima and T. Ichihashi, Nature (London) **363**, 603 (1993).

[8] *Carbon Nanotubes: Advanced Topics in the Synthesis, Structure, Properties, and Applications*, edited by A. Jorio, G. Dresselhaus, and M. S. Dresselhaus (Springer, Berlin, 2008).

[9] T. Ando, J. Phys. Soc. Jpn. **66**, 1066 (1997).

[10] C. D. Spataru, S. Ismail-Beigi, L. X. Benedict, and S. G. Louie, Phys. Rev. Lett. **92**, 077402 (2004).

[11] F. Wang, G. Dukovic, L. E. Brus, and T. F. Heinz, Science **308**, 838 (2005).

[12] J. Maultzsch, R. Pomraenke, S. Reich, E. Chang, D. Prezzi, A. Ruini, E. Molinari, M. S. Strano, C. Thomsen, and C. Lienau, Phys. Rev. B **72**, 241402(R) (2005).

[13] G. Dukovic, F. Wang, D. Song, M. Y. Sfeir, T. F. Heinz, and L. E. Brus, Nano Lett. **5**, 2314 (2005).

[14] W. Wegscheider, L. N. Pfeiffer, M. M. Dignam, A. Pinczuk, K. W. West, S. L. McCall, and R. Hull, Phys. Rev. Lett. **71**, 4071 (1993).

[15] D. Moses, J. Wang, A. J. Heeger, N. Kirova, and S. Brazovski, Proc. Natl. Acad. Sci. U.S.A. **98**, 13496 (2001).

[16] S. M. King, D. Dai, C. Rothe, and A. P. Monkman, Phys. Rev. B **76**, 085204 (2007).

[17] V. Perebeinos, J. Tersoff, and Ph. Avouris, Phys. Rev. Lett. **94**, 027402 (2005); **94**, 086802 (2005).

[18] J. Jiang, R. Saito, K. Sato, J. S. Park, Ge. G. Samsonidze, A. Jorio, G. Dresselhaus, and M. S. Dresselhaus, Phys. Rev. B **75**, 035405 (2007).

[19] X. Qiu, M. Freitag, V. Perebeinos, and Ph. Avouris, Nano Lett. **5**, 749 (2005).

[20] S. G. Chou, F. Plentz, J. Jiang, R. Saito, D. Nezich, H. B. Ribeiro, A. Jorio, M. A. Pimenta, Ge. G. Samsonidze, A. P. Santos, M. Zheng, G. B. Onoa, E. D. Semke, G. Dresselhaus, and M. S. Dresselhaus, Phys. Rev. Lett. **94**, 127402 (2005).

[21] H. Htoon, M. J. O'Connell, S. K. Doorn, and V. I. Klimov, Phys. Rev. Lett. **94**, 127403 (2005).

[22] Y. Miyauchi and S. Maruyama, Phys. Rev. B **74**, 035415 (2006).

[23] A. Nish, J.-Y. Hwang, J. Doig, and R. J. Nicholas, Nat. Nanotechnol. **2**, 640 (2007).

[24] M. S. Arnold, S. I. Stupp, and M. C. Hersam, Nano Lett. **5**, 713 (2005).

[25] M. S. Arnold, A. A. Green, J. F. Hulvat, S. I. Stupp, and M. C. Hersam, Nat. Nanotechnol. **1**, 60 (2006).

[26] O. Kiowski, K. Arnold, S. Lebedkin, F. Hennrich, and M. M. Kappes, Phys. Rev. Lett. **99**, 237402 (2007).

[27] O. N. Torrens, M. Zheng, and J. M. Kikkawa, Phys. Rev. Lett. **101**, 157401 (2008).

[28] K. Yanagi, Y. Miyata, and H. Kataura, Appl. Phys. Express **1**, 034003 (2008).

[29] See EPAPS Document No. E-PRBMDO-79-111915 for the sample preparation details. For more information on EPAPS, see http://www.aip.org/pubservs/epaps.html

[30] S. M. Bachilo, M. S. Strano, C. Kittrell, R. H. Hauge, R. E. Smalley, and R. B. Weisman, Science **298**, 2361 (2002).

[31] T. Inoue, K. Matsuda, Y. Murakami, S. Maruyama, and Y. Kanemitsu, Phys. Rev. B **73**, 233401 (2006).

[32] V. Perebeinos, J. Tersoff, and Ph. Avouris, Nano Lett. **5**, 2495 (2005).

[33] I. B. Mortimer and R. J. Nicholas, Phys. Rev. Lett. **98**, 027404 (2007).

[34] J. Shaver, J. Kono, O. Portugall, V. Krstić, G. L. J. A. Rikken, Y. Miyauchi, S. Maruyama, and V. Perebeinos, Nano Lett. **7**, 1851 (2007).

[35] R. Saito, A. Jorio, A. G. Souza Filho, G. Dresselhaus, M. S. Dresselhaus, and M. A. Pimenta, Phys. Rev. Lett. **88**, 027401 (2001).

[36] K. Sato, R. Saito, Y. Oyama, J. Jiang, L. G. Cançado, M. A. Pimenta, A. Jorio, Ge. G. Samsonidze, G. Dresselhaus, and M. S. Dresselhaus, Chem. Phys. Lett. **427**, 117 (2006).

[37] M. A. Pimenta, G. Dresselhaus, M. S. Dresselhaus, L. G. Cancado, A. Jorio, and R. Saito, Phys. Chem. Chem. Phys. **9**, 1276 (2007).

[38] E. B. Barros, R. B. Capaz, A. Jorio, Ge. G. Samsonidze, A. G. Souza Filho, S. Ismail-Beigi, C. D. Spataru, S. G. Louie, G. Dresselhaus, and M. S. Dresselhaus, Phys. Rev. B **73**, 241406(R) (2006).